Metal–Organic Frameworks |Hot Paper|

A Nanotubular Metal–Organic Framework with a Narrow Bandgap from Extended Conjugation**

M. Menaf Ayhan,[b] Ceyda Bayraktar,[b] Kai Bin Yu,[c] Gabriel Hanna,[d] A. Ozgur Yazaydin,[c] Yunus Zorlu,*[b] and Gündoğ Yücesan*[a]

Abstract: A one-dimensional nanotubular metal–organic framework (MOF) [Ni(Cu-H_4TPPA)]·2$(CH_3)_2NH_2^+$ (H_8TPPA = 5,10,15,20-tetrakis[*p*-phenylphosphonic acid] porphyrin) constructed by using the arylphosphonic acid H_8TPPA is reported. The structure of this MOF, known as **GTUB-4**, was solved by using single-crystal X-ray diffraction and its geometric accessible surface area was calculated to be 1102 $m^2 g^{-1}$, making it the phosphonate MOF with the highest reported surface area. Due to the extended conjugation of its porphyrin core, **GTUB-4** possesses narrow indirect and direct bandgaps (1.9 eV and 2.16 eV, respectively) in the semiconductor regime. Thermogravimetric analysis suggests that **GTUB-4** is thermally stable up to 400 °C. Owing to its high surface area, low bandgap, and high thermal stability, **GTUB-4** could find applications as electrodes in supercapacitors.

Metal–organic frameworks (MOFs) are microporous materials that contain well-defined micropores composed of organic and inorganic surfaces.[1–9] They have been used in applications ranging from gas adsorption, sequestration of greenhouse gases,[10,11] catalysis,[12,13] magnetism,[14–17] drug delivery,[18,19] cosmetics,[20] food packaging and transportation,[21,22] proton conductive membranes,[23,24] and electrical conduction.[16,25–28] Although thousands of MOFs have been reported in the literature, the structural diversity of MOFs, MOF linker core geometries, and different metal-binding functional groups have not been fully exploited yet. Recently, two new families of MOFs have emerged, which employ phosphonic and phosphinic acids as metal-binding units, in contrast with the conventional MOFs that contain carboxylates and azolates.[29–32] Phosphonic acids are able to support extremely rich metal-binding modes, while phosphinic acids have carboxylate-like metal-binding modes.[33] The presence of d-orbitals in the phosphorus atom can give rise to rich electronic interactions, which have resulted in completely different geometries compared to those of conventional MOFs.[29–32] Owing to the higher strength of the C–P and P–O bonds compared to R-C=O bonds, phosphonate MOFs exhibit higher thermal and chemical stabilities compared to conventional MOFs.[15,34,35] To the best of our knowledge, the total number of microporous phosphonate MOFs is currently less than 0.001% of the total number of reported MOFs.[29–34] Nevertheless, they have already opened new vistas in catalysis,[36,37] proton conductivity,[23,37,38] and biological applications.[39,40]

One of the commonly studied properties in MOF research is semiconductivity.[25–28] Traditional carboxylate MOFs are generally known to be insulators with bandgaps outside of the semiconducting regime.[25,26] The majority of the known semiconductive MOFs are based on *ortho*-diimine, *ortho*-dihydroxy, and azolate linkers; however, due to their very conservative metal-binding units, further structural development has been limited.[1,25–28] Therefore, new metal-binding units that give rise to high structural diversity and semiconductivity are needed. In this direction, the phosphonic acid metal-binding unit (R-PO_3^{2-}) containing phosphorus, which is a good conductor and has a negative charge that is evenly distributed over the three tetrahedronally oriented oxygen atoms, has shown great promise. We have recently shown that the presence of phosphonic acids promotes electron delocalization in the one-dimensional inorganic building unit (IBU) of the phosphonate MOF TUB75, which is composed of polyaromatic 1,4-naphthalenediphosphonic acid linkers and one-dimensional copper-containing IBUs and has a narrow bandgap of 1.4 eV.[16] To build upon this work, in this study, we used a conjugated tetratopic linker, H_8-TPPA, to synthesize another narrow bandgap phosphonate MOF, namely [Ni(Cu-H_4TPPA)]·2$(CH_3)_2NH_2^+$ (**GTUB-4**, where TUB stands for Technische Universität Berlin

[a] *Dr. G. Yücesan*
Technische Universität Berlin, Department of Food Chemistry and Toxicology, Gustav-Meyer-Allee 25, 13355 Berlin (Germany)
E-mail: yuecesan@tu-berlin.de

[b] *Dr. M. M. Ayhan, C. Bayraktar, Dr. Y. Zorlu*
Department of Chemistry, Faculty of Science
Gebze Technical University, 41400, Gebze, Kocaeli (Turkey)
E-mail: yzorlu@gtu.edu.tr

[c] *K. B. Yu, Dr. A. O. Yazaydin*
Department of Chemical Engineering, University College London
London WC1E 7JE (UK)

[d] *Dr. G. Hanna*
University of Alberta, Department of Chemistry
116 St. and 85 Ave., Edmonton, Alberta T6G 2R3 (Canada)

[**] *A previous version of this manuscript has been deposited on a preprint server (https://doi.org/10.26434/chemrxiv.11920026.v1).*

Supporting information and the ORCID identification number(s) for the author(s) of this article can be found under: https://doi.org/10.1002/chem.202001917.

and G stands for Gebze), which has a unique one-dimensional microporous tubular structure with a very high geometric accessible surface area of 1102 $m^2 g^{-1}$ and low indirect bandgap of 1.90 eV.

Due to the rich metal-binding modes of organophosphonates, the rational synthesis of phosphonate MOFs into predefined one-, two-, and three-dimensional frameworks has been a great challenge.[29–36] Previously, phosphonate monoesters mimicking the carboxylate metal binding were used to generate microporous MOFs.[41,42] Recently, we developed a new strategy to retain mono-deprotonated R-PO_3H^{-1} in hydrothermal reactions via a pH-controlled synthesis.[43,44] The R-PO_3H^{-1} metal-binding unit also provides carboxylate-like metal binding to generate predictable phosphonate MOFs. In this study, we aimed to attain the simplest metal-binding modes with the tetratopic, structurally rigid, and planar phosphonic acid H_8TPPA (which contains a conjugated porphyrin core), whose phosphonic acid moieties are separated by ≈90° from one other. Thus, when H_8-TPPA is coordinated to molecular IBUs in the simplest 1.100 mode (in Harris notation[45]), they are expected to create square or rectangular void spaces. In this connection, our goal was to create H_4TPPA^{4-} (in which each phosphonate arm is mono-deprotonated) to achieve the 1.100 metal-binding mode. In addition, we aimed to create an extended one-dimensional conjugated system that facilitates the conduction of electrons. To achieve this, we performed a low-temperature synthesis in DMF to promote the formation of molecular IBUs, as a high-temperature hydrothermal synthesis could provide enough energy to form one-dimensional or two-dimensional IBUs. Furthermore, in a square planar coordination environment, the high energy d^9 electrons of Cu^{II} can support conductive behavior in MOFs.[25] Inside a porphyrin core, Cu^{II} usually adopts a square planar coordination environment. Therefore, we adapted the Pd-catalyzed Arbuzov reaction to synthesize metal-free H_8-TPPA. Due to the large ionic radius of the Pd atom, it does not readily incorporate into the porphyrin ring, allowing one to incorporate other metal atoms into the porphyrin core.[39,46] Later, we introduced square planar Cu^{II} into H_8-TPPA pyrrole ring to synthesize **Cu-H_8TPPA** (the deprotonated pyrrole hydrogens are omitted in this formula). **GTUB-4** was synthesized in a DMF/H_2O and phenylphosphonic acid (modulator) mixture at 80 °C for 24 h, giving rise to long dark red needle-like crystals in high yield (see Supporting Information for experimental details). These carefully controlled conditions were required to achieve the simplest 1.100 phosphonate metal-binding modes.

The structure of **GTUB-4** was solved using X-ray crystallography. As seen in Figure 1, **GTUB-4** has a one-dimensional tubular structure. Each tube consists of a central rectangular void channel (see Figures 1 a and b) and two different hexagonal voids on the sides, top, and bottom of the tube (see Figure 1 c and d). The phosphonate metal-binding groups in **GTUB-4** have 1.100 metal-binding modes (the simplest type of metal-binding mode), where a Ni^{II} atom forms two coordinate covalent bonds and two ionic bonds with the phosphonate groups of the H_8TPPA linker. As mentioned earlier, this was achieved under well-controlled pH, temperature, and solvent conditions—the three variables that can be tuned to explore the large structural space of phosphonate MOFs. The presence of dimethylammonium cations and the acidic nature of **GTUB-4** suggest that increasing the basicity of **GTUB-4** environment could lead to further deprotonation of the phosphonic acids and, in turn, variations in the structure and properties. The crystal structure of **GTUB-4** reveals that it contains a simple IBU, namely octahedral nickel metal centers coordinated to the four phosphonic acid metal-binding groups of H_8-TPPA. As seen in Figure 1 A and B, the basal plane of octahedral Ni exclusively connects the Cu-H_4TPPA^{4-} linkers, while the apical positions of Ni are occupied by two water molecules. Furthermore, as seen in Figure 2 A–C, **GTUB-4's** nanotubes are held together through hydrogen bonds with the water molecules located at the apical positions of the octahedral Ni^{II}. Therefore, **GTUB-4** can also be viewed as a three-dimensional hydrogen-bonded framework constructed from one-dimensional MOF nanotubes. Figure 2 D shows that the two distinct MOF nanotubes are packed at 41.87° relative to each other, leading to growth in two different directions. As the tubular structure of

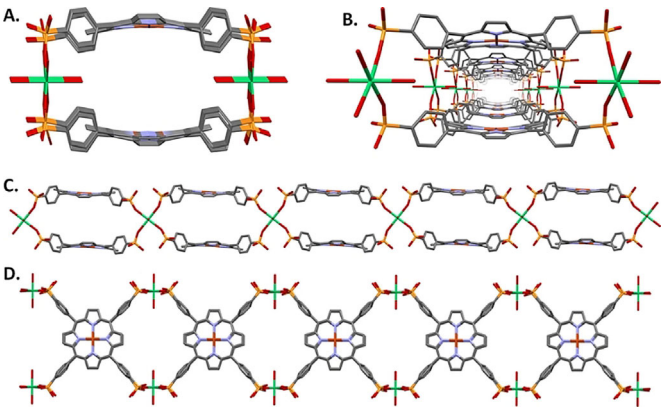

Figure 1. a) Edge view of the rectangular void channel of **GTUB-4**. b) Perspective view of the rectangular void channel. c) Side-top view of tubular structure and its hexagonal sieves. d) Another side view facing the CuH_4TPPA^{4-} building unit with square void channels.

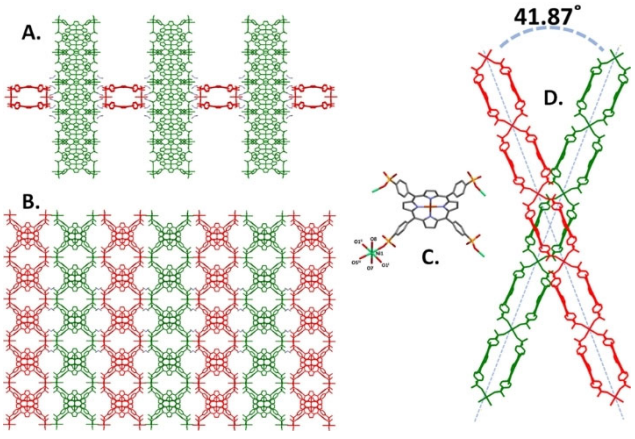

Figure 2. a, b, d) Different views of the cross-packed **GTUB-4** tubes in the crystal lattice. c) Cu-H_4TPPA^{4-} metal-binding modes with Ni.

GTUB-4 is composed of three distinct pore sites (see Figure 1 A, C, and D), the textural properties of **GTUB-4** were characterized with molecular simulations (see the Supporting Information for details). Our calculations yielded a specific pore volume of 0.425 $cm^3 g^{-1}$, a geometric accessible surface area of 1102 $m^2 g^{-1}$, and pores of ≈5 Å in diameter (see Figure S7).

The structure of **GTUB-4** shown in Figure 1 D suggests that H_8-TPPA conjugation extends over the mono-deprotonated tetrahedral phosphonate metal-binding unit R-P=O(OH)O^{-1}, in which the phosphonate electrons could delocalize over the tetrahedral geometry. In light of these results, we used solid-state diffuse reflectance spectroscopy (DRS) to estimate the optical bandgap of **GTUB-4** (see Figure 3). The indirect optical bandgap of **GTUB-4** was found to be 1.9 eV (see the Supporting Information for details).[47–49] The narrowness of the bandgap is likely due to the extended conjugation mediated by the mono-deprotonated phosphonate metal-binding unit.

The presence of metal ions typically increases the thermal stability of MOFs compared to that of the linkers due to the additional covalent and ionic bonding opportunities in MOFs. Thus, we studied the thermal behaviors of H_8-TPPA, Cu-H_8TPPA, and **GTUB-4** by thermogravimetric analysis (TGA). As seen in Figure S3, the TGA curve obtained under N_2 from the hand-picked **GTUB-4** crystals indicates that the solvent and water molecules evaporate from **GTUB-4** until 100 °C. The second step of ≈11.1% weight loss corresponds to the evaporation of dimethylammonium cations in the crystal lattice (12.3% calculated). The third step of ≈28.8% weight loss between ≈400 °C and ≈650 °C corresponds to the evaporation of nearly half of the organic components of H_8TPPA (52% calculated). The decomposition of **GTUB-4** continues above 900 °C, suggesting that **GTUB-4** might be converted into thermally stable phosphides above 650 °C.[50]

In summary, we reported a nanotubular MOF, **GTUB-4**, which was constructed using the highly conjugated H_8-TPPA linker. The strict pH and temperature control enabled the formation of a one-dimensional tubular structure with a geometric accessible surface area of 1102 $m^2 g^{-1}$. The conjugated porphyrin core and electron delocalization around the phosphonate metal-binding unit are believed to enhance the conjugation along the 1D structure. This results in a narrow bandgap of 1.9 eV, suggesting that **GTUB-4** is a semiconductor. We were able to selectively introduce square planar Cu^{II} with high energy electrons into the porphyrin core of **GTUB-4**, where the linker connectivity is achieved via octahedral Ni centers. The thermal decomposition pattern of **GTUB-4** indicates that it is thermally stable up to 400 °C, after which the organic components of the porphyrin core decompose. The presence of water at the apical position of the octahedral Ni site suggests the possibility of post-synthetic modifications of **GTUB-4**. Due to its narrow bandgap and high surface area, **GTUB-4** could be used as an electrode material in the next generation of supercapacitors. We are currently working on merging the one-dimensional tubular channels to synthesize a three-dimensional version of **GTUB-4**.

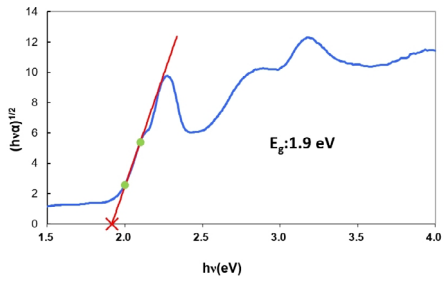

Figure 3. Estimation of the indirect bandgap of **GTUB-4** via Tauc plotting of the DRS spectrum.

Acknowledgements

The authors would like to thank the DFG and TÜBİTAK (117Z383) for funding our work. Open access funding enabled and organized by Projekt DEAL.

Conflict of interest

Gündoğ Yücesan has a pending patent protecting some of the presented results.

Keywords: high surface area · ligand design · metal–organic frameworks · nanotubes · semiconductive MOFs

[1] H. Li, E. Eddaoudi, M. O'Keeffe, O. M. Yaghi, *Nature* **1999**, *402*, 276–279.
[2] A. Schneemann, V. Bon, I. Schwedler, I. Senkovska, S. Kaskel, R. A. Fischer, *Chem. Soc. Rev.* **2014**, *43*, 6062–6096.
[3] G. Férey, C. Mellot-Draznieks, C. Serre, F. Millange, *Acc. Chem. Res.* **2005**, *38*, 217–225.
[4] H. Furukawa, K. E. Cordova, M. O'Keeffe, O. M. Yaghi, *Science* **2013**, *341*, 1230444.
[5] H. C. Zhou, J. R. Long, O. M. Yaghi, *Chem. Rev.* **2012**, *112*, 673–674.
[6] N. Stock, S. Biswas, *Chem. Rev.* **2012**, *112*, 933–969.
[7] Y. V. Kaneti, S. Dutta, S. A. Hossain, M. J. Shiddiky, K.-L. Tung, F.-K. Shieh, C.-K. Tsung, K. C.-W. Wu, Y. Yamauchi, *Adv. Mater.* **2017**, *29*, 1700213.
[8] G. Gumilar, Y. V. Kaneti, J. Henzie, S. Chatterjee, J. Na, B. Yuliarto, N. Nugraha, A. Patah, A. Bhaumik, Y. Yamauchi, *Chem. Sci.* **2020**, *11*, 3644–3655.
[9] C. Wang, J. Kim, J. Tang, M. Kim, H. Lim, V. Malgras, J. You, Q. Xu, J. Li, Y. Yamauchi, *Chem* **2020**, *6*, 19–40.
[10] O. M. Yaghi, M. O'Keeffe, N. W. Ockwig, H. K. Chae, M. Eddaoudi, J. Kim, *Nature* **2003**, *423*, 705–714.
[11] N. Hanikel, M. S. Prévot, F. Fathieh, E. A. Kapustin, H. Lyu, H. Wang, N. J. Diercks, T. G. Glover, O. M. Yaghi, *ACS Cent. Sci.* **2019**, *5*, 1699–1706.
[12] A. Dhakshinamoorthy, Z. Li, H. Garcia, *Chem. Soc. Rev.* **2018**, *47*, 8134–8172.
[13] D. Yang, B. C. Gates, *ACS Catal.* **2019**, *9*, 1779–1798.
[14] G. Mínguez Espallargas, E. Coronado, *Chem. Soc. Rev.* **2018**, *47*, 533–557.
[15] Y. Zorlu, D. Erbahar, A. Çetinkaya, A. Bulut, T. S. Erkal, A. O. Yazaydin, J. Beckmann, G. Yücesan, *Chem. Commun.* **2019**, *55*, 3053–3056.
[16] K. Siemensmeyer, C. A. Peeples, P. Tholen, F. J. Schmitt, B. Çoşut, G. Hanna, G. Yücesan, *Adv. Mater.* **2020**, *32*, 2000474.
[17] C. Yang, R. Dong, M. Wang, P. S. Petkov, Z. Zhang, M. Wang, P. Han, M. Ballabio, S. A. Bräuninger, Z. Liao, J. Zhang, F. Schwotzer, E. Zschech, H. H. Klauss, E. Cánovas, S. Kaskel, M. Bonn, S. Zhou, T. Heine, X. Feng, *Nat. Commun.* **2019**, *10*, 3260.
[18] P. Horcajada, R. Gref, T. Baati, P. K. Allan, G. Maurin, P. Couvreur, G. Férey, R. E. Morris, C. Serre, *Chem. Rev.* **2012**, *112*, 1232–1268.

[19] K. J. Hartlieb, D. P. Ferris, J. M. Holcroft, I. Kandela, C. L. Stern, M. S. Nassar, Y. Youssry, J. Botros, J. F. Stoddart, *Mol. Pharmaceutics* **2017**, *14*, 1831 – 1839.
[20] K. J. Hartlieb, A. W. Peters, T. C. Wang, P. Deria, O. K. Farha, J. T. Hupp, J. F. Stoddart, *Chem. Commun.* **2017**, *53*, 7561 – 7564.
[21] P. L. Wang, L. H. Xie, E. A. Joseph, J. R. Li, X. O. Su, H. C. Zhou, *Chem. Rev.* **2019**, *119*, 10638 – 10690.
[22] B. Zhang, Y. Luo, K. Kanyuck, G. Bauchan, J. Mowery, P. Zavalij, *J. Agric. Food Chem.* **2016**, *64*, 5164 – 5170.
[23] S. S. Bao, G. K. H. Shimizu, L. M. Zheng, *Coord. Chem. Rev.* **2019**, *378*, 577 – 594.
[24] D. A. Levenson, J. Zhang, P. M. J. Szell, D. L. Bryce, B. S. Gelfand, R. P. S. Huynh, N. Fylstra, G. K. H. Shimizu, *Chem. Mater.* **2020**, *32*, 679 – 687.
[25] L. Sun, M. G. Campbell, M. Dinca, *Angew. Chem. Int. Ed.* **2016**, *55*, 3566 – 3579; *Angew. Chem.* **2016**, *128*, 3628 – 3642.
[26] L. S. Xie, G. Skorupskii, M. Dinca, *Chem. Rev.* **2020**, *120*, 8536 – 8580.
[27] D. Sheberla, J. C. Bachman, J. S. Elias, C. J. Sun, Y. Shao-Horn, M. Dincă, *Nat. Mater.* **2017**, *16*, 220 – 224.
[28] A. J. Rieth, Y. Tulchinsky, M. Dincă, *J. Am. Chem. Soc.* **2016**, *138*, 9401 – 9404.
[29] G. Yücesan, Y. Zorlu, M. Stricker, J. Beckmann, *Coord. Chem. Rev.* **2018**, *369*, 105 – 122.
[30] S. J. Shearan, N. Stock, F. Emmerling, J. Demel, P. A. Wright, K. D. Demadis, M. Vassaki, F. Costantino, R. Vivani, S. Sallard, I. R. Salcedo, A. Cabeza, M. Taddei, *Crystals* **2019**, *9*, 270.
[31] P. Bhanja, J. Na, T. Jing, J. Lin, T. Wakihara, A. Bhaumik, Y. Yamauchi, *Chem. Mater.* **2019**, *31*, 5343 – 5362.
[32] P. Tholen, Y. Zorlu, J. Beckmann, G. Yücesan, *Eur. J. Inorg. Chem.* **2020**, 1542 – 1554.
[33] J. Hynek, P. Brázda, J. Rohlíček, M. G. S. Londesborough, J. Demel, *Angew. Chem. Int. Ed.* **2018**, *57*, 5016 – 5019; *Angew. Chem.* **2018**, *130*, 5110 – 5113.
[34] K. J. Gagnon, H. P. Perry, A. Clearfield, *Chem. Rev.* **2012**, *112*, 1034 – 1054.
[35] C. Gao, J. Ai, H. Tian, D. Wub, Z. Sun, *Chem. Commun.* **2017**, *53*, 1293 – 1296.
[36] X. Chen, Y. Peng, X. Han, *Nat. Commun.* **2017**, *8*, 2171.
[37] B. S. Gelfand, R. P. S. Huynh, R. K. Mah, G. K. H. Shimizu, *Angew. Chem. Int. Ed.* **2016**, *55*, 14614 – 14617; *Angew. Chem.* **2016**, *128*, 14834 – 14837.
[38] J. M. Taylor, R. K. Mah, I. L. Moudrakovski, C. I. Ratcliffe, R. Vaidhyanathan, G. K. H. Shimizu, *J. Am. Chem. Soc.* **2010**, *132*, 14055 – 14057.
[39] M. Maares, M. M. Ayhan, K. B. Yu, A. O. Yazaydin, K. Harmandar, H. Haase, J. Beckmann, Y. Zorlu, G. Yücesan, *Chem. Eur. J.* **2019**, *25*, 11214 – 11217.
[40] Y. Zorlu, C. Brown, C. Keil, M. M. Ayhan, H. Haase, R. B. Thompson, I. Lengyel, G. Yücesan, *Chem. Eur. J.* **2020**, 26, 11129 – 11134.
[41] S. S. Iremonger, J. Liang, R. Vaidhyanathan, I. Martens, G. K. H. Shimizu, T. D. Daff, M. Z. Aghaji, S. Yeganegi, T. K. Woo, *J. Am. Chem. Soc.* **2011**, *133*, 20048 – 20051.
[42] J. M. Taylor, R. Vaidhyanathan, S. S. Iremonger, G. K. H. Shimizu, *J. Am. Chem. Soc.* **2012**, *134*, 14338 – 14340.
[43] A. Bulut, Y. Zorlu, M. Wörle, A. Çetinkaya, H. Kurt, B. Tam, A. Ö. Yazaydın, J. Beckmann, G. Yücesan, *ChemistrySelect* **2017**, *2*, 7050 – 7053.
[44] A. Bulut, Y. Zorlu, E. Kirpi, A. Çetinkaya, M. Wörle, J. Beckmann, G. Yücesan, *Cryst. Growth Des.* **2015**, *15*, 5665 – 5669.
[45] R. A. Coxall, S. G. Harris, D. K. Henderson, S. Parsons, P. A. Tasker, R. E. P. Winpenny, *Dalton Trans.* **2000**, 2349 – 2356.
[46] G. Yucesan, V. Golub, C. J. O'Connor, J. Zubieta, *CrystEngComm* **2004**, *6*, 323 – 325.
[47] J. Tauc, R. Grigorovici, A. Vancu, *Phys. Status Solidi* **1966**, *15*, 627 – 637.
[48] J. Tauc, *Optical Properties of Solids*, Abeles, North Holland, Amsterdam, **1972**.
[49] E. A. Davis, N. F. Mott, *Philos. Mag.* **1970**, *22*, 0903 – 0922.
[50] R. Zhang, P. A. Russo, M. Feist, P. Amsalem, N. Koch, N. Pinna, *ACS Appl. Mater. Interfaces* **2017**, *9*, 14013 – 14022.

Manuscript received: April 20, 2020
Revised manuscript received: June 3, 2020
Accepted manuscript online: June 5, 2020
Version of record online: ■■ ■■, 0000

COMMUNICATION

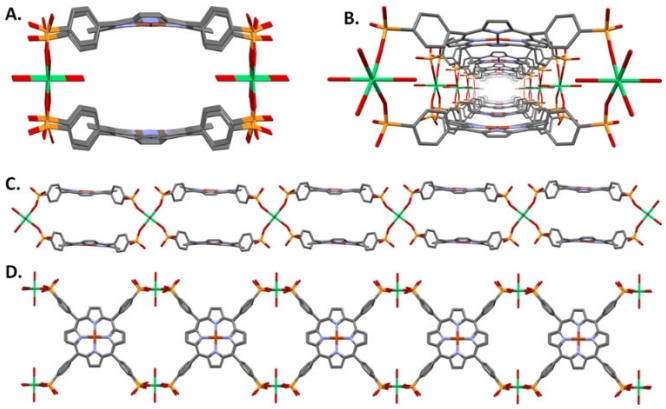

A 1D nanotubular MOF, GTUB-4, was constructed by using the highly conjugated arylphosphonic acid H_8-TPPA. The structure of this metal–organic framework (MOF) was solved by using single-crystal X-ray. GTUB-4 is characterized by high surface area and, due to the extended conjugation of its porphyrin core, possesses narrow indirect and direct bandgaps in the semiconductor regime. Owing to its high surface area, low band gap, and high thermal stability, GTUB-4 could find applications as electrode material in supercapacitors.

Metal–Organic Frameworks

M. M. Ayhan, C. Bayraktar, K. B. Yu, G. Hanna, A. O. Yazaydin, Y. Zorlu, G. Yücesan**

■■ – ■■

A Nanotubular Metal–Organic Framework with a Narrow Bandgap from Extended Conjugation